Secondary ion mass spectroscopic studies of the atomic geometry of GaAs(110)

Rik Blumenthal, S. K. Donner, J. L. Herman, Rajender Trehan,[a] K. P. Caffey, Ehud Furman,[b] and Nicholas Winograd
Department of Chemistry, The Pennsylvania State University, University Park, Pennsylvania 16802

B. D. Weaver
Department of Physics, The Pennsylvania State University, University Park, Pennsylvania 16802

(Received 1 February 1988; accepted 25 April 1988)

The atomic geometry of the GaAs(110) surface has been determined by shadow-cone enhanced desorption. Ga^+ secondary ion yields were analyzed without extensive calculations or assumptions of structure except that the second and all lower layer atoms are at bulk lattice sites. The structure determined from this simple analysis shows excellent qualitative agreement with most preceding models. The surface As atomic position is determined to be displaced laterally 1.28 Å toward the second layer Ga atom and is relaxed away from the surface by 0.69 Å, while the surface Ga atom is displaced 0.37 Å laterally in the same direction as the As atom and compressed 0.45 Å toward the surface. The resulting chain rotation is 29.3° and both surface As bond lengths are determined to be lengthened. A detailed discussion of the shadow-cone enhanced desorption method of structure analysis is presented along with areas of possible refinement. Also presented is a description of our experimental apparatus which was developed for the *in situ* characterization of molecular-beam epitaxially grown surfaces.

I. INTRODUCTION

The structure of the GaAs(110) surface has been extensively scrutinized. The earliest attempts at determining the atomic geometry of this surface[1,2] involved elastic low-energy electron diffraction (ELEED) experiments with visual fitting of experimental spot intensity versus voltage curves to curves calculated for model structures. These studies led to the development of bond length conserving models where the surface reconstructs by a simple rotation of the surface chain without allowing any bond length changes. This chain can be seen as a vertical zig–zag of alternating atoms in the top view of Fig. 1. The results of these analyses have proven to be surprisingly accurate yielding a chain rotation angle between 27° and 34.8° with a slightly better fit at higher rotation angles. These early ELEED studies were followed by calculations of the GaAs(110) surface electronic structure,[3–5] the results of which were consistent with the original ideas about the bond rotation but which postulated a lateral translation of the chain to match the ordering of surface states observed by angle-resolved photoemission.[6,7] As a consequence of the lateral displacements the rigid bond length conserving models gave way to a bond length relaxation model. Isochromat spectroscopy[8,9] confirmed the ordering of the surface states, and the bond length relaxation model gained acceptance. The newer model spurred more in-depth calculations to determine their compatibility with ELEED data.[10] Results from these calculations suggested that the sensitivity of ELEED to lateral displacements was poor, and it was concluded that in light of this fact both models fit the data equally well, and a newer best fit model was proposed. As a pathology of the data fitting routine a model having a 7° surface chain rotation was found to result in a minimum in the fitting parameter, but was discounted when integrated beam intensities were considered in the fitting routine. In the next few years, the first ion surface studies of structure were performed[11–13] with differing conclusions. High-energy ion channeling latched onto the 7° model and medium energy ion scattering confirmed the original bond length conserving model. This spurred further in-depth treatement of the surface by ELEED[14,15] which suggested that although some agreement with the high-energy ion channeling studies could be reached, the quality of the fit

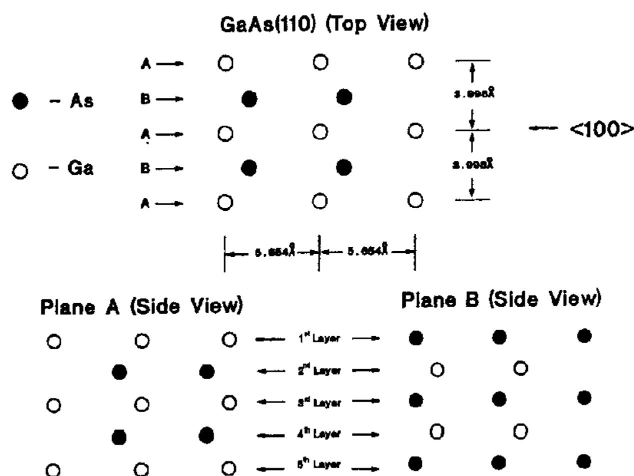

FIG. 1. A top view of the GaAs(110) crystal surface (upper) is depicted along with side views of the two dissimilar planes in the ⟨100⟩ directions labeled A (lower left) and B (lower right).

 0734-211X/88/041444-07$01.00 © 1988 American Vacuum Society

was not nearly as good as that for the refined model.[10] Further photoemission studies[16] also revealed a 27° chain rotation model with small parallel displacements. The purpose of this study is to apply our novel structural analysis, requiring no assumptions of model structure or extensive calculations, to the GaAs(110) surface as a test of its sensitivity to surface reconstructions, and as a direct measure of lateral displacements.

In the past, our research has focused on the angular distributions of secondary ions and neutrals to examine surface geometries.[17] This approach requires extensive molecular dynamics simulations of individual ion impact events and a comparison of the experimental ion distributions to calculated distributions. Furthermore, an effective interaction potential is required for use in these simulations. In the case of metals, a Moliere potential, the repulsive part, coupled with a Morse potential, the attractive part, are fit to match the bulk thermodynamic features of the crystal. This choice of potential has proven sufficient to match experimental data.[18] It should be noted that this potential has spherical symmetry, and cannot be used for crystals displaying tetrahedral coordination. Recently, a potential has been developed for Si,[18] which is currently being utilized in full dynamics simulations of ion–solid interactions, but no effort has been made to adapt it for use with GaAs.

Recently, Chang[19] demonstrated that if the ion beam incidence is oriented properly, then an atom in the top layer may deflect ions toward an atom in a lower layer; thereby increasing the momentum transfer into the surface region and increasing the total sputter yield. The focusing of ion incidence flux onto and away from lower layers has been well established in terms of shadow cones, regions of space behind an atom where no flux is incident. This new technique is analogous to impact-collision ion scattering spectrometry (ICISS),[20,21] except that instead of detecting the scattered primary ion, secondary ions are detected. Shadow-cone enhanced desorption has been successfully applied to elucidating the surface reconstruction of Ag(110)[22] and determining the bond length of Cl adsorbed on Ag(110).[23]

In this work we present an independent determination of the GaAs(110) surface structure using shadow-cone enhanced desorption. This technique is particularly well-suited to studies of covalent materials because of the large interplanar spacings in these crystals. Using a novel data analysis technique, we determine a 29.3° surface chain rotation, accompanied by bond length changes of − 3.9%, + 9.9%, and + 28.4% for the surface to Ga, surface to As, and Ga to As distances, respectively. These bond lengths do represent a significant difference from previous models, and an analysis of possible reasons is presented. In addition, we describe a new experimental apparatus which allows these types of experiments to be performed on films grown by molecular-beam epitaxy (MBE) which can be transferred under UHV conditions from the growth chamber to the analysis chamber.

II. EXPERIMENTAL

Our experimental apparatus integrates a commercial MBE growth chamber and a surface analysis system equipped with techniques aimed toward the characterization of the first few atomic layers of the sample. To achieve the dual purpose of operating an electronics-grade growth facility and of studying the films prepared without the use of capping or exposure to air, a third chamber is incorporated to provide sample introduction and transfer abilities. In this

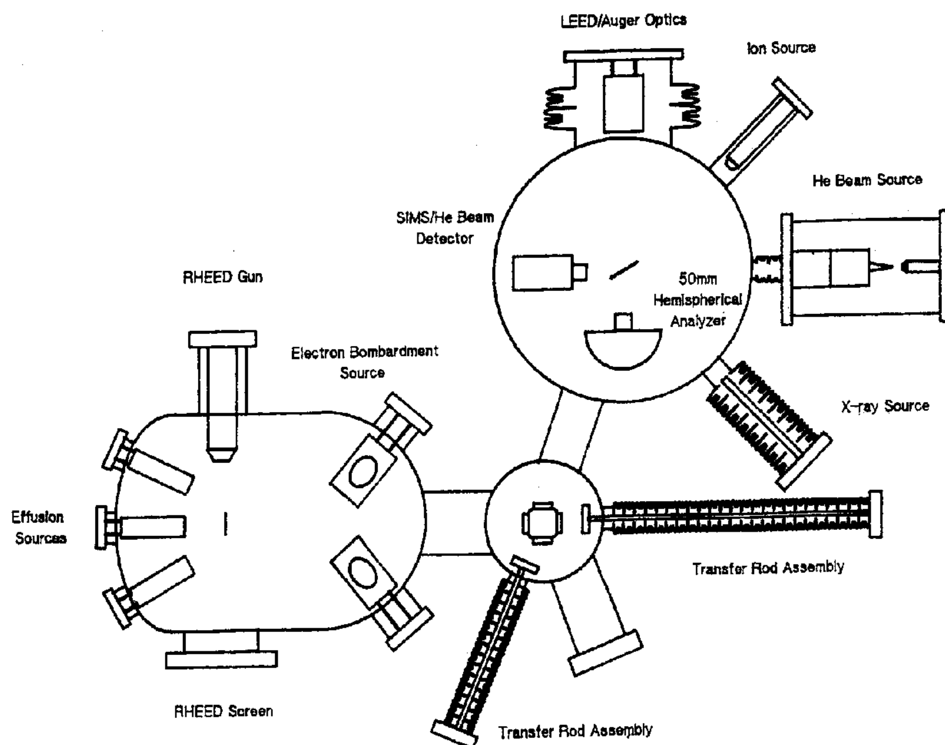

FIG. 2. Schematic drawing of experimental apparatus consisting of a Riber 2300R&D MBE growth chamber with effusion sources and electron bombardment sources (lower left), sample introduction and preparation chamber (lower right), and the surface analysis chamber (upper right). The secondary ion/He beam detector (see Fig. 3) and 50 mm hemispherical energy analyzer are mounted to a rotating flange on the chamber bottom to allow the angle between any of the sources and either detector to be set arbitrarily.

paper, we will describe the complete experimental apparatus (see Fig. 2), although the MBE part of the system is not required to prepare the GaAs(110) surface.

A. MBE growth chamber

A Riber 2300 R&D growth chamber is used to prepare samples for study. The chamber is equipped for use with up to eight effusion sources and two electron bombardment sources. All effusion sources are directed at a common sample growth position while the two electron bombardment sources are directed at a second growth position. The entire chamber is lined with liquid nitrogen shrouds and is pumped by a 400 l/s ion pump and a titanium sublimation pump. The chamber is also equipped with a standard reflection high-energy electron diffraction system to monitor growth conditions.

Samples can be prepared in the form of 2-in. wafers, or fractions thereof, for mounting with indium on a cylindrical molybdenum block for handling. This molybdenum block has six pins protruding outward beyond the edge, one set of three pins for a manipulator and the other for a transfer system. The sample temperature is regulated during growth by radiative heating from behind the block, and the temperature is monitored by a W–Re thermocouple placed inside a cavity of the block at the center of rotation. The manipulator also has an ion gauge positioned so that it can be rotated into growth positions for direct beam flux measurements. At present, the chamber is equipped with three effusion ovens (Ga, Al, and As).

B. Surface analysis chamber

To allow the maximum flexibility in experimental design, the surface analysis chamber has an 18-in. diameter rotating flange serving as the chamber bottom. To allow some element of compactness the chamber has multiple experimental levels. The multiple levels serve a second function by allowing the use of a single quadrupole mass analyzer for both secondary ion mass spectroscopy (SIMS) and atom scattering experiments. Commensurate with the complexity of the chamber design, the sample manipulator employed was custom designed to suit the many needs of the wide variety of experiments possible in this one chamber.

As previously stated, the entire chamber bottom rotates on a pair of bearings, and the vacuum seal is made with the use of three Teflon rings which remain stationary as the highly polished metal of the flange rotates inside them. These three seals define two differential stages of pumping. The first is pumped by a trapped rotary pump, and the second is pumped by a 20 l/s ion pump. The greatest benefit to be gained from the rotating flange is that if the experimental detectors are mounted to the flange, then the angle of detection can be varied as desired for a particular experiment.

At present, the chamber is equipped with a Leybold–Heraeus rare gas ion source, a VSW x-ray source, Perkin–Elmer LEED/AUGER optics, a Fenn-type nozzle atom beam source, a VSW 50 mm hemispherical energy analyzer, and an extranuclear quadrupole mass analyzer. The chamber pump is a CTI cryopump, and the typical base pressure achieved after baking is $<8\times10^{-11}$ Torr.

To allow for 360° rotation of the flange and equipment mounted on it, the ion source has been recessed 9 in. from chamber center on a permanent nipple. The x-ray source has been placed on a bellows assembly so it can be withdrawn from its experimental position at 1 in. from chamber center to a position completely clear of the chamber. The LEED/AUGER optics have been modified to a view-from-behind configuration. To achieve this goal the metal collector/phosphor screen was removed and replaced with a transparent Sb-doped SnO coated glass screen; the exterior dimensions of the electron gun were reduced; and a viewport was added to the center of the mounting flange. To allow lid rotation and insertion of the optics into the chamber, the length of the assembly was adjusted and the unit is mounted on a bellows assembly.

The atom beam source employed in diffraction experiments consists of three differentially pumped stages: the nozzle exhaust region (stage 1), the chopper chamber (stage 2), and the collimation chamber (stage 3). The atom beam source has been described in detail elsewhere.[24]

Both the hemispherical energy analyzer and the quadrupole mass analyzer are mounted on the rotating flange. The entrance to the energy analyzer is on the same experimental level as the ion and x-ray sources. The entrance to the cross-beam ionizer of the quadrupole is on the same level as the atom beam source. Since the same quadrupole is used as the SIMS detector the ionizer was modified to allow ions to be injected vertically down into the quadrupole. To deflect SIMS ions from the ion and x-ray source level a 90° spherical sector energy analyzer is positioned with its entrance in the experimental level and its exit pointing vertically down into the quadrupole. Three element lenses are used at both the entrance and exits to insure maximum transmission. At the front of the entrance lens is a 1.5-mm aperture to define an experimental detection angle half-width of ~0.7° (see Fig. 3).

The sample manipulator is a five axis design. The transla-

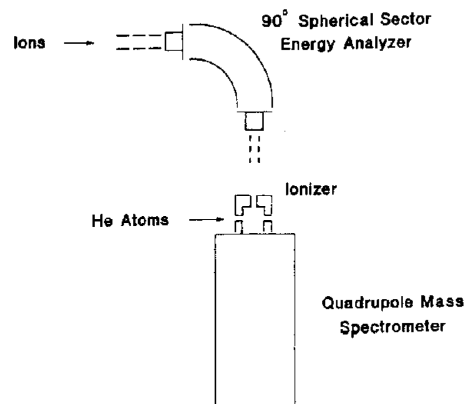

FIG. 3. Secondary ion/He beam detector utilizes a single quadrupole mass analyzer for both purposes. Secondary ions are focused into a 90° spherical sector energy analyzer for energy selection and deflection to the quadrupole axis where further focusing into the quadrupole is accomplished with another lens and the cross beam ionizer. He beams are ionized and focused directly into the quadrupole at a lower chamber level.

tion modules in the plane of the experiment allow ± 1 in. of travel and the vertical translator has a 19 in. stroke. The rotation mechanisms provide 360° continuous independent rotations in either the polar (in the plane of the experiment) or azimuthal (in the plane of the sample) directions. The sample is heated by electron bombardment from behind the mounting block, and cooled by contact with a liquid-nitrogen reservoir pneumatically moved in or out of contact with the block. To reduce vibrations at the sample induced by the 42 in. insertion length of the rotary motion feedthrough, four 0.25 in. steel rods run along the majority of the length and terminate at a common bearing. This five rod assembly has proved to be adequate vibrational isolation even though the chamber is cryopumped.

The manipulator polar and azimuthal rotations as well as the vertical translation are under the control of a DEC 11/2 computer. All data acquisitions, either phase-sensitive detection of atom beams or pulse counting of secondary ions, are taken with the same computer.

C. Preparation and sample introduction chamber

As previously mentioned the efficient use of both the MBE and analysis chambers and the maintenance of high-quality vacuums in these chambers at all times requires the presence of a third chamber for sample introduction, transfer, and management. This chamber is equipped with both of the transfer rod assemblies. The transfer rod assemblies are essentially rotary motion feedthroughs mounted on 30 in. bellows for the insertion through this chamber and to the manipulator of one of the other chambers. The transfer mechanism is actually very simple. It is designed opposite handed with respect to manipulator sample locks. Samples are transferred by rotating the transfer system rod to unlock one set of block pins while simultaneously locking the other set of pins into position. The manipulator in this chamber is designed to hold up to four blocks at one time and each holder is equipped with its own heating assembly and thermocouple.

D. Sample preparation

Oriented and polished GaAs(110) wafers were obtained from M/A Com Laser Diodes Inc. Samples were degreased by successive rinses of trichloroethane, acetone, and methanol, chemically etched in a 5:1:1 solution of H_2SO_4, H_2O, and H_2O_2, and mounted on a molybdenum block with indium. The samples were further prepared for study by repeated cycles of ion bombardment and annealing at 595° for 20 min. Sample cleanliness was verified frequently by SIMS and occasionally by Auger electron spectroscopy and no sign of impurities was ever detected for a surface prepared in this manner. Surface order was verified by LEED and He diffraction.

III. CALCULATIONS

The goal of this effort is to generate an experimental model of the GaAs(110) surface which can be analyzed without the need for extensive computer simulations. This goal is possible using two straight forward calculations which yield a nearly model-independent surface structure determination.

First, it is necessary to evaluate the shadow-cone shape appropriate for the collision of a 3000-eV Ar^+ ion with a Ga or As surface atom. These shapes are quite accurately known and have been calculated using established procedures.[25] The only adjustable parameter in this formalism is the Firsov screening length which we chose to be 0.8 in accord with most previously reported values.[26]

The second set of calculations is required to determine the set of atomic positions that could give rise to an interaction of a shadow-cone tail with a surface atom at an experimentally determined angle. This calculation is equivalent to rotating the shadow cone to the experimental angle, and tracing the set of points through which the origin of the shadow cone travels when one edge is constrained to contain the position of the atom onto which flux is being focused. The above procedures are easily carried out in a matter of seconds even on the most primitive personal computers.

IV. RESULTS AND DISCUSSION

The Ga^+ SIMS intensities in the ⟨100⟩ and ⟨$\bar{1}$00⟩ azimuths are plotted as a function of ion beam incidence angle in Figs. 4(a) and 4(b), respectively. For each spectrum, the angle designated as + 90° corresponds to an ion beam incidence parallel to the surface. The angle between the source and detector is set to ~25° resulting in a loss of meaningful signal at ~ − 65° as the detector crosses the surface plane. Signal may still persist beyond this angle but is the result of sputtering from the side of the sample. Ion beam current during all experiments was kept below 100 pA focused into a 1-mm-diam spot size. Spectra were collected in a 30-min scan resulting in a total ion fluence of 5×10^{13} ions/cm^2 (the atomic density of this surface is 8×10^{14} atoms/cm^2).

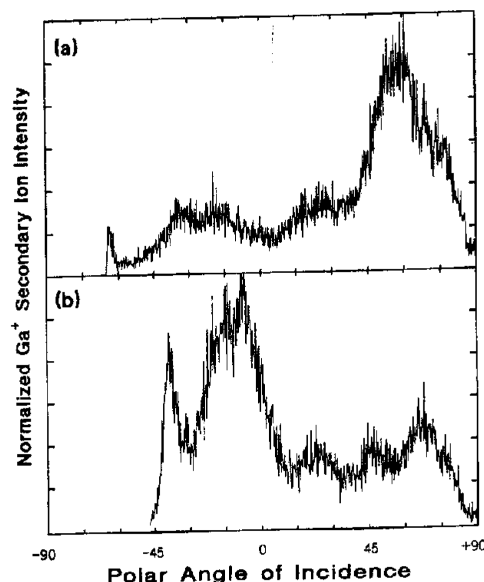

FIG. 4. Ga^+ secondary ion yields are plotted as a function of ion beam incidence angle is varied. In (a) [(b)] ion beam incidence is along the ⟨100⟩ [⟨$\bar{1}$00⟩] direction and parallel to the surface is designated as + 90°.

The degree of surface damage created by Ar^+ ion bombardment during a typical experiment has been evaluated by He beam scattering studies which is known to be very sensitive to defect formation and requires excellent surface order for a specular scattering peak to be observed.[27] In our experiments, the specular scattering intensity is ~4% of the incidence He flux after annealing and drops to 0.6% after an ion dose equal to the experimental ion dose. The persistance of a significant amount of the scattered intensity suggests only a small fraction of the surface is being altered during a typical experiment. No degradation of LEED patterns was observed at these low-surface damage levels. Finally, to examine the sensitivity of the measurements to surface damage, scans from $+90°$ to $-70°$ were compared to scans from $-70°$ to $90°$ and no significant differences could be found in the features, but a small loss of intensity (~20%–30%) at the end of each scan was found. It should also be noted that the end of the low-dose scans did not resemble scans obtained at higher ion doses, which show none of the fine features used in data analysis.

Analysis of data is made in terms of sharp increases in secondary Ga^+ intensities as the atoms in the crystal are exposed to ion flux. A list of all identified features of each spectrum is made in Table I. Analysis of the atomic positions of the surface Ga and As atoms is made independently in the *A* and *B* planes, respectively (see Fig. 1). This treatment is justified by the fact that a 2-Å spacing exists between the *A* and *B* planes which greatly exceeds the shadow-cone radius for 3 keV Ar^+ at distances along the shadow cone of 50 Å. This results in negligible focusing of ions from one plane to the other in the experimental conditions.

For the purposes of this discussion it is necessary to make certain definitions. The atom that is the origin of the shadow-cone will be referred to as the shadow-cone source and the atom onto which flux is being focused will be referred to as the shadow-cone reference. Analysis of the geometry is made using the following procedure. All possible features, sharp increases in signal, are identified at one time, and the angles of the maximum of the increase are tabulated before any analysis is carried out. An individual feature is assigned a reference atom (a second or lower layer atom assumed to be in a bulk lattice position) in a best guess method. This restriction of subsurface geometry is the only one made and is reasonable considering that the largest displacement in a previous model was 0.06 Å.[10] A second feature is then assigned to a reference atom, in the plane under analysis. Each assignment is used to calculate its own set of possible source atom positions. The results of these calculations are then overlayed and the point of their crossing is identified as a tentative surface atom position.

Tentative surface atomic positions must then be tested by searching the tabulated list of features for a third (fourth, fifth, etc.) assignment which is calculated as having the tentative surface atom position as its source. If no confirming assignments can be made a new pair of initial assignments are made and the whole procedure is repeated.

It is possible, on occasion, to find only one or two possible confirming assignments. These "false" assignments are of two differing natures. The first is where the real interaction is occurring with a source in the second or third layer and a reference in the same or a lower layer. These false assignments result in bulk lattice sites being determined in the surface layer, and are easy to identify and skip. The second type of false assignment is the chance that three or four random assignments might result in sets of source atom positions that happen to cross at one point. This possibility is not large, but this type of false surface position determination was observed during this analysis. As further evidence of the rarity of this type of false assignment, no cases were found where four or more assignments pointed to a single source position, except for the case of the two atomic positions determined as the surface Ga and As atomic positions below.

The results of this analysis are shown graphically in Figs. 5(a) and 5(b). The calculated sets of source positions for all assignments made in the determination of the surface atomic position in each plane are shown in each figure. In each case, at least eight assignments pointed to a common source position. The last obstacle is to evaluate the remaining features not assigned in this analysis. Once again features resulting from bulk lattice interactions can be readily identified by calculating the angles of interaction from the second and lower layers with the lower layers, and assigning these calculated angles to observed features. Features identified in this manner are labeled bulk in Table I. The remaining features are few in number and probably represent multiple scattering interactions where the incident ion flux is focused once by the surface and then focused again by a lower layer atom before it impinges on the reference atom. This type of interaction cannot be examined within the binary collision approximation which is integrally assumed in any shadow cone analysis.

The final determination of surface atomic positions is

TABLE I. Listing of features identified from the Ga^+ secondary ion spectra.

	Angles(deg)			
Spectrum	Plane *A* [c]	Plane *B* [d]	Bulk	Unassigned
(100) [a]	73.8	65.6	85.6	42.8
	68.9	52.4	77.4	32.8
	48.4	48.4	65.6	−6.4
	27.6		60.8	−14.8
	24.2		48.4	
			24.2	
			17.8	
			−9.4	
			−19.8	
($\bar{1}$00) [b]	52.0	31.8	78.0	72.1
	44.2	30.4	65.6	35.8
	19.0	25.8	44.2	11.6
		0.0	25.8	
		−20.6	19.0	
			7.8	
			−7.4	
			−14.8	
			−27.0	

[a] See Fig. 4(a).
[b] See Fig. 4(b).
[c] Shown graphically in Fig. 5(a).
[d] Shown graphically in Fig. 5(b).

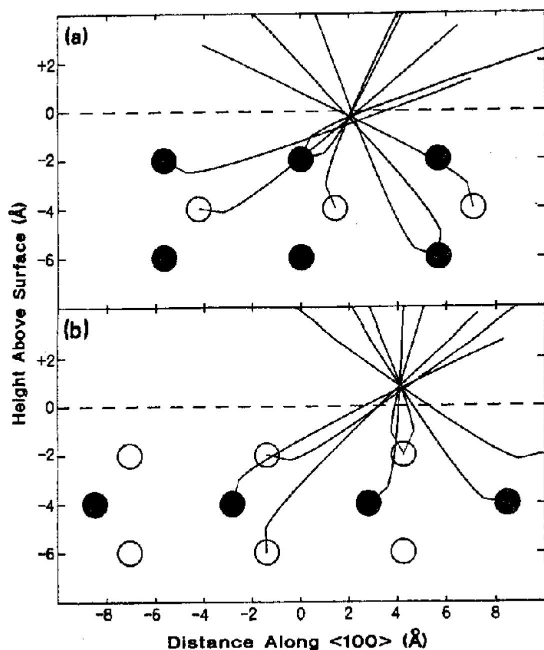

FIG. 5. (a) [(b)] represents the plane labeled *A* (*B*) in Fig. 1 with the first layer stripped off. Each curve represents the calculated set of surface atom positions that can result in an experimentally observed interaction. The region of the crossing of these curves represents the experimentally determined Ga (As) surface atom position.

made from Figs. 5(a) and 5(b). In plane *A* [see Fig. 5(a)], six of the eight assignments result in a crossing point at (1.78, − 0.45), or a lateral displacement of 0.37 Å away from the second layer As atom and a compression into the crystal of 0.30 Å. The diagram also yields a random error in the position of ± 0.1 Å. The *B* plane [Fig. 5(b)] shows seven of the eight curves crossing at a single position (4.11,0.69). These displacements correspond to a lateral shift in the same direction of the Ga of 1.28 Å and a relaxation away from the surface of 0.69 Å. The same random error can be assigned to the As atomic position.

This structure represents a rotation of the surface chain by 29.3° and a relaxation of all bond lengths. The Ga surface atom to second layer As atom bond length is contracted by 3.7%, while the As surface atom to second layer Ga atom bond is relaxed by 9.9%, and the Ga surface to As surface bond length is relaxed 33.7%. In comparison with existing models the rotation of the surface chain is in excellent agreement with most other structures,[1–10] but bond lengthening of the observed magnitude has not previously been reported. It is possible that the observed bond lengthenings are the consequence of unknown systematic error in the data analysis. Our approach is quite novel and has yet to be tested on a variety of systems for systematic errors.

In this study, the angle at which the shadow cone sweeps across an atom is characterized by a sharp increase in signal. The assignment of the angle of this rise was made at the peak of the rise, due to its easy identification and reproducibility. However, it is equally reasonable to assign other parts of the feature to the angle of interaction. We find that an improper identification of the angle of interaction could yield a systematic change in the determination of bond lengths. At this stage, we do not believe that these effects are significantly influencing the results of our analysis. For example, analysis of interactions with sources in the second layer yield the correct second layer atomic positions within our current ± 0.1 Å error limit.

V. CONCLUSION

A new experimental and theoretical approach to the determination of surface structure has been proposed and tested for GaAs(110). The atomic structure of the GaAs(110) surface has been determined by shadow-cone enhanced desorption in an analysis requiring no extensive calculations or assumptions except that the second and lower layer atoms remain at bulk lattice sites. The structure determined is in excellent qualitative agreement with previous studies,[1–5,10,17] although the bond lengths determined by this method are relaxed.

The data analysis technique developed is especially well-suited for the study of covalent crystals due to the large interplanar spacings common to their structures. We look forward to future application of this methodology for structure determinations on a variety of semiconductor surfaces. For example, this approach should be particularly powerful for *in situ* examination of MBE surfaces prepared in our system. Finally, it will be of considerable interest to see if our initial data analysis routines can be improved upon by removing the uncertainty in the assignment of interaction angles to the features. This can be achieved by a variety of methods. Two obvious ones are to utilize more sophisticated modeling techniques to determine the angle of maximum-flux on the reference atom and to improve the angular resolution and noise level by signal averaging. In general, we believe this methodology is especially powerful for the determination of the complex structures typical of semiconductor surfaces, since the atomic coordinates can be computed without the need for initial assumptions.

ACKNOWLEDGMENTS

The authors gratefully thank D. R. Frankl for his invaluable contributions to the design and use of the atomic beam source. The authors also wish to acknowledge the financial support of the National Science Foundation, the Office of Naval Research, and the IBM Corporation.

[a] Present address: Department of Chemistry, Rutgers University, Piscataway, NJ 08855-0939.
[b] Present address: ADA, P. O. Box 2250, Heifa, Israel (Dept. 23).

[1] A. R. Lubinsky, C. B. Duke, B. W. Lee, and P. Mark, Phys. Rev. Lett. **36**, 1058 (1976).
[2] C. B. Duke, A. R. Lubinsky, B. W. Lee, and P. Mark, J. Vac. Sci. Technol. **13**, 761 (1976).
[3] D. J. Chadi, J. Vac. Sci. Technol. **15**, 631 (1978).
[4] D. J. Chadi, J. Vac. Sci. Technol. **15**, 1244 (1978).
[5] J. J. Barton, W. A. Goddard III, and T. C. McGill, J. Vac. Sci. Technol. **16**, 1178 (1979).
[6] A. Huijser, J. van Laar, and T. L. van Rooy, Phys. Lett. A. **65**, 335 (1978).
[7] J. A. Knapp and G. J. Lapeyre, J. Vac. Sci. Technol. **13**, 757 (1976).
[8] V. Dose, H.-J. Gossmann, and D. Straub, Phys. Rev. Lett. **47**, 608 (1981).
[9] V. Dose, H.-J. Gossmann, and D. Straub, Surf. Sci. **117**, 387 (1982).
[10] G. B. Duke, S. L. Richardson, and A. Paton, Surf. Sci. **127**, 1135 (1983).

[11]H.-J. Gossmann and W. M. Gibson, Surf. Sci. **139**, 239 (1984).
[12]H.-J. Gossmann and W. M. Gibson, J. Vac. Sci. Technol. B **2**, 343 (1984).
[13]L. Smit, T. E. Derry, and J. F. van der Veen, Surf. Sci. **150**, 245 (1985).
[14]C. B. Duke and A. Paton, Surf. Sci. **164**, L797 (1985).
[15]C. B. Duke and A. Paton, J. Vac. Sci. Technol B **2**, 327 (1984).
[16]C. Mailhoit, C. B. Duke, and Y. C. Chang, Phys. Rev. B **30**, 1109 (1984).
[17]N. Winograd, in *Desorption Mass Spectrometry*, Am. Chem. Soc. Symp. Ser. No. 291, edited by P. A. Lyon (American Chemical Society, Washington D.C., 1985), pp. 83–96.
[18]B. J. Garrison, in Ref. 17, pp. 43–55.
[19]C. C. Chang, Ph.D. thesis, The Pennsylvania State University, 1987.
[20]M. Aono, C. Oshima, S. Zaima, S. Otani, and Y. Ishizawa, Jpn. J. Appl. Phys. **20**, 1829 (1981).
[21]M. Aono, Nucl. Instrum. Methods B **2**, 374 (1984).
[22]C. C. Chang and N. Winograd (to be submitted).
[23]C. C. Chang, G. P. Malafsky, and N. Winograd, J. Vac. Sci. Technol. A **5**, 981 (1987).
[24]B. D. Weaver and D. R. Frankl, Rev. Sci. Instrum. **58**, 2115 (1987).
[25]I. Stensgaard, L. C. Feldman, and P. J. Silverman, Surf. Sci. 77, 513 (1978).
[26]J. A. Yarmoff and R. S. Williams, Surf. Sci. **127**, 461 (1983).
[27]G. Cosma and B. Poelsema, Appl. Phys. A **38**, 153 (1985).